

## Analysis of $\pi N \rightarrow \pi\pi N$ in Chiral Perturbation Theory

---

**Dmitrij Siemens\***

*Ruhr-Universität Bochum*

*E-mail:* [dmitrij.siemens@rub.de](mailto:dmitrij.siemens@rub.de)

The reaction  $\pi N \rightarrow \pi\pi N$  is studied up to next-to-leading order in the frameworks of manifestly covariant and heavy-baryon chiral perturbation theory. In addition, the effects of explicit  $\Delta(1232)$  degrees of freedom are analyzed. The relevant low-energy constants are determined from fits to low-energy total cross section data and predictions for total cross sections at higher energies as well as differential cross sections are made.

*The 8th International Workshop on Chiral Dynamics, CD2015 \*\*\**

*29 June 2015 - 03 July 2015*

*Pisa, Italy*

---

\*Speaker.

## 1. Introduction

Chiral perturbation theory ( $\chi$ PT) was originally formulated by Weinberg [1] and later extended and applied to study the dynamics of the meson and baryon sector [2, 3, 4]. Since then,  $\chi$ PT has extensively been used in the single-baryon sector [5, 6, 7] and various extensions appeared over the years (see Ref. [7] for more details).

In this paper, the reaction  $\pi N \rightarrow \pi\pi N$  is analyzed from threshold up to the  $\Delta$  resonance region using various formulations of  $\chi$ PT. This process was of historical interest as a possible candidate to extract the  $\pi\pi$  scattering lengths [10, 11, 12] and is nowadays an excellent testing ground for  $\chi$ PT due to the involvement of three pions in the initial and final states, the relatively high energies involved and the strong couplings to close-by resonances. This makes the reaction  $\pi N \rightarrow \pi\pi N$  particularly well suited for studying the role of relativistic effects, unitarity and the  $\Delta$  isobar.

All these arguments encourage a revision of the reaction  $\pi N \rightarrow \pi\pi N$  in the framework of  $\chi$ PT. The reader is referred to Refs. [12, 13, 14, 15, 16] for previous analyses. This paper strongly borrows from Ref. [17].

## 2. Effective Lagrangian and Invariant Amplitudes

The so-called small scale expansion (SSE) or  $\varepsilon$ -expansion is employed throughout this work. Pion-nucleon dynamics is described at tree level by the covariant effective chiral Lagrangian consisting of the following pieces

$$\mathcal{L}_{\text{eff}} = \mathcal{L}_{\pi\pi}^{(2)} + \mathcal{L}_{\pi N}^{(1)} + \mathcal{L}_{\pi N}^{(2)} + \mathcal{L}_{\pi\Delta}^{(1)} + \mathcal{L}_{\pi\Delta}^{(2)} + \mathcal{L}_{\pi N\Delta}^{(1)} + \mathcal{L}_{\pi N\Delta}^{(2)}, \quad (2.1)$$

where the superscripts refer to the chiral dimension with the expansion parameter [8]

$$\varepsilon \in \left\{ \frac{q}{\Lambda_\chi}, \frac{M_\pi}{\Lambda_\chi}, \frac{\Delta}{\Lambda_\chi} \right\}, \quad (2.2)$$

and a full list of terms is given in detail in Ref. [19].

To study the role of relativistic effects, all calculations are also performed in the framework of heavy-baryon (HB)  $\chi$ PT. In this approach, in addition to  $\Lambda_\chi$ , the nucleon mass  $m_N$  is treated as a hard scale as well and the expansion parameter in Eq. (2.2) is extended accordingly. The reader is referred to Refs. [8, 9] for more details on the HB expansion in the pion-nucleon-delta sector.

The necessary formulas to decompose the  $T$ -matrix for the reaction  $\pi N \rightarrow \pi\pi N$  into invariant amplitudes and their relations to observables like total and differential cross sections are given in Refs. [14, 15] for both chiral approaches.

## 3. Tree-level contributions to the scattering amplitude

The diagrams contributing at order  $\varepsilon^1$  and  $\varepsilon^2$  in both frameworks are shown in Figure 1. While the leading-order diagrams are solely dependent on the well-established LECs  $F_\pi$ ,  $g_A$  and  $h_A$ , the next-to-leading-order diagrams depend additionally on the LECs  $c_i$  from  $\mathcal{L}_{\pi N}^{(2)}$  or  $b_i$  from  $\mathcal{L}_{\pi N\Delta}^{(2)}$ . The LECs  $c_i$  can be fixed from an analysis of pion-nucleon scattering.

It has to be emphasized that the  $\Delta$  isobar, due to its appearance as an unstable particle, needs a special treatment in the resonance region  $p^2 \sim m_\Delta^2$ . In this region the  $\Delta$  propagator in the amplitudes has to be dressed [18]. While this dressing is only necessary in the resonance region, we employed the dressed  $\Delta$  propagator for all kinematical regions and in all diagrams.

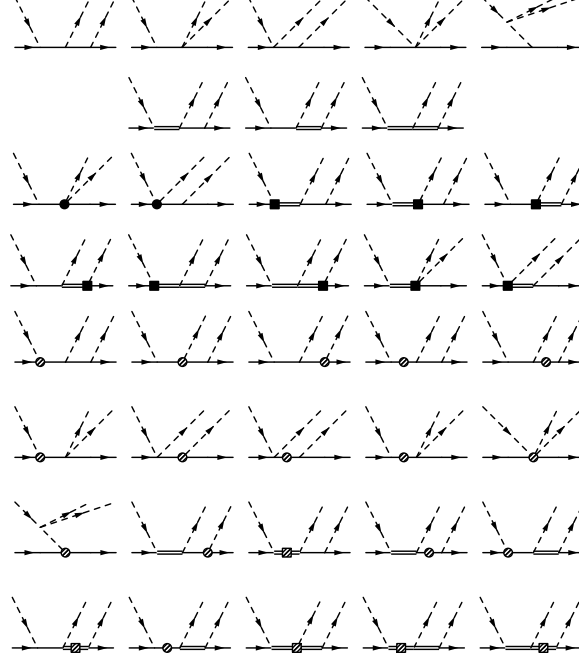


**Figure 1:** Leading-order and next-to-leading-order diagrams for the reaction  $\pi N \rightarrow \pi\pi N$ . Nucleons and pions are denoted by solid and dashed lines, respectively.  $\Delta$  is denoted by a double solid line. The filled blob (filled square) denotes an insertion of the  $c_i$ - ( $b_i$ -) vertices. The additional next-to-leading-order graphs contributing in the HB framework are denoted by the shaded blob/square. Crossed diagrams are not shown.

#### 4. Fitting Procedure

As explained in the previous section, the leading-order Lagrangian depends on various well-known LECs. Following values are used in the calculations:  $M_\pi = 139.57$  MeV,  $F_\pi = 92.4$  MeV,  $m_N = 938.27$  MeV,  $g_A = 1.26$ ,  $\Delta = 294$  MeV,  $\Gamma = 118$  MeV,  $h_A = 1.34$  and  $g_1 = 2.27$  (both large- $N_c$  predictions). The LECs  $c_i$  entering the next-to-leading-order graphs are taken from pion-nucleon scattering [20, 21] and their values in the  $\Delta$ -full and  $\Delta$ -less approach are collected in Table 1. The values for the additional LECs  $b_3$ ,  $b_4$ ,  $b_5$ ,  $b_6$  entering at order  $\varepsilon^2$  are unknown and their

$\Delta$	$c_1$	$c_2$	$c_3$	$c_4$	$\Delta$	$c_1$	$c_2$	$c_3$	$c_4$
KH	-0.95	1.90	-1.78	1.50	KH	-0.75	3.49	-4.77	3.34
GW	-1.41	1.84	-2.55	1.87	GW	-1.13	3.69	-5.51	3.71

**Table 1:** LECs  $c_i$  from the pion-nucleon sector in a  $\Delta$ -full ( $\Delta$ ) and  $\Delta$ -less ( $\Delta$ ) theory. All values are given in  $\text{GeV}^{-1}$ .

determination will be discussed in the following. Note that the LECs  $b_3$  and  $b_6$  can be absorbed

into the other LECs and are redundant in the static limit [25]. These shifts were performed in the HB as well as in the covariant amplitudes such that a meaningful comparison of both approaches is possible.

All fits were performed to all five physical channels simultaneously and only the total cross section data with  $T_\pi < 250$  MeV was used. This data is taken from the compilation [22] and from [23, 24, 26]. The resulting values for the LECs  $b_i$  using the KH and GW sets of LECs  $c_i$  as input are listed in Table 2.

Fit	$c_i$	$b_4 + b_5$	$b_4 - b_5$	$b_3 + b_6$	$b_3 - b_6$	$\chi^2/\text{dof}$
HB	KH	$16.00 \pm 0.37$	$-7.99 \pm 5.72$	—	—	9.63
	GW	$15.99 \pm 0.37$	$-8.42 \pm 5.77$	—	—	9.65
Cov	KH	$4.97 \pm 0.29$	$-17.71 \pm 12.22$	$0.39 \pm 0.86$	$1.60 \pm 7.62$	3.40
	GW	$4.34 \pm 0.29$	$-18.24 \pm 10.77$	$0.70 \pm 0.76$	$1.41 \pm 6.38$	3.47

**Table 2:** LECs determined from global fits to the total cross section data ( $T_\pi < 250$  MeV) at next-to-leading-order using the KH and GW sets of LECs  $c_i$  as input. The values of LECs  $b_i$  are given in units of  $\text{GeV}^{-1}$ .

The fits show a strong anticorrelation between the LECs  $b_4$  and  $b_5$ . While a reliable extraction of the linear combination  $b_4 + b_5$  is possible, the linear combination  $b_4 - b_5$  can only be given with a very large uncertainty of about 100%. The LECs  $b_3$  and  $b_6$  are strongly anticorrelated in the covariant approach as well.

The significance of relativistic effects in the reaction  $\pi N \rightarrow \pi\pi N$  is very well demonstrated in the strong reduction of  $\chi^2/\text{dof}$  from  $\sim 9.6$  in the HB approach to  $\sim 3.4$  in covariant  $\chi PT$ . A further indication that the energies up to  $T_\pi = 250$  MeV employed in the fit are probably beyond the applicability range of the HB approach at order  $\varepsilon^2$ , are the unnaturally large values of the linear combination  $b_4 + b_5$  in HB $\chi PT$ , while the same linear combination in covariant  $\chi PT$  is of reasonably natural size.

## 5. Predictions

Total cross sections at higher energies and also other observables like differential cross sections can now be predicted with the LECs collected in Table 2. The predictions in both frameworks, HB and covariant  $\chi PT$ , will allow us to estimate the importance of relativistic effects in the reaction under consideration. Note that all predictions at next-to-leading-order are visualized by bands instead of lines. The bands are produced by taking both sets of LECs, denoted by KH and GW in Table 2. This allows us to give a rough uncertainty estimation associated with the input stemming from the pion-nucleon system.

In Figure 2, the predictions for the total cross section with energies up to  $T_\pi \simeq 400$  MeV are shown for four different approaches, covariant  $\Delta$ -full, HB  $\Delta$ -full, covariant  $\Delta$ -less and HB  $\Delta$ -less  $\chi PT$ . In total agreement with the observations made in the previous section, the covariant predictions agree way better with the data than the HB ones. The next-to-leading-order HB predictions without  $\Delta$  underestimate the data, whereas the HB predictions with explicit  $\Delta$  overestimate the data for  $T_\pi > 300$  MeV. The explicit treatment of the  $\Delta$  in the covariant case is mainly noticeable in the

upper two channels, whereas the covariant predictions for the other three channels are quite similar in both cases,  $\Delta$ -full and  $\Delta$ -less.

In Figure 3, the covariant predictions for  $d\sigma/dM_{\pi\pi}^2$  and  $d\sigma/dt$  are presented for the two channels  $\pi^- p \rightarrow \pi^+ \pi^- n$  and  $\pi^+ p \rightarrow \pi^+ \pi^+ n$ . Recalling that the total cross section in the  $\pi^+ \pi^-$  channel is very accurately predicted at order  $\varepsilon^2$ , both single-differential cross sections are also well described in the  $\Delta$ -full approach. The  $\Delta$ -less results at order  $Q^2$  strongly underestimate the single-differential cross sections, which is fully in line with the observed underprediction of the total cross section. In contrast, the single-differential cross sections in the  $\pi^+ \pi^+$ -channel are poorly predicted at both orders,  $Q^2$  and  $\varepsilon^2$ . Recalling that the total cross section is significantly overpredicted in both approaches, the observed large deviations for the single-differential cross sections should not be surprising.

Finally, a comparison with the previous calculations within the covariant [15] and HB [14] frameworks shows consistent predictions of total and differential cross sections for both  $\Delta$ -less approaches. A comparison with the calculation of Ref. [13] points out that their leading-order results with explicit  $\Delta$  and Roper give a similar description of the total cross sections as our next-to-leading-order  $\Delta$ -full results. Note that they additionally included the Roper resonance explicitly and that there is no strict power counting underlying their calculations.

## 6. Summary and outlook

In this paper an analysis of the reaction  $\pi N \rightarrow \pi\pi N$  at tree level up to next-to-leading order using the  $\Delta$ -full and  $\Delta$ -less HB and manifestly covariant formulations of  $\chi PT$  was performed. The main results are:

- Total cross section data of all five physically accessible channels with  $T_\pi < 250$  MeV was fitted in order to determine the low-energy constants  $b_i$ . Due to strong anticorrelations, only the linear combinations  $b_4 + b_5$  and  $b_3 + b_6$  were reliably determined. They are found to be of natural size in the covariant approach.
- The description of the experimental data is clearly superior in the covariant subleading calculation compared to the HB one. Furthermore, the explicit treatment of the  $\Delta$  leads to an improvement in the description of the data.

This work is going to be extended in the near future by calculations at the next-higher orders in the chiral expansion. The aim is to test the convergence of the chiral expansion and also to constrain further higher order LECs by a combined analysis of the reactions  $\pi N \rightarrow \pi N$  and  $\pi N \rightarrow \pi\pi N$ .

## Acknowledgments

This work was supported by the DFG (SFB/TR 16, ‘‘Subnuclear Structure of Matter’’), the European Community-Research Infrastructure Integrating Activity ‘‘Study of Strongly Interacting Matter’’ (acronym HadronPhysics3, Grant Agreement n. 283286) under the Seventh Framework Programme of EU, and the ERC project 259218 NUCLEAREFT and the Ruhr University Research School PLUS, funded by Germany’s Excellence Initiative [DFG GSC 98/3].

## References

- [1] S. Weinberg, *Phenomenological Lagrangians*, *Physica A* **96** (1979) 327.
- [2] J. Gasser and H. Leutwyler, *Chiral Perturbation Theory to One Loop*, *Annals Phys.* **158** (1984) 142.
- [3] J. Gasser and H. Leutwyler, *Chiral Perturbation Theory: Expansions in the Mass of the Strange Quark*, *Nucl. Phys. B* **250** (1985) 465.
- [4] J. Gasser, M. E. Sainio and A. Svarc, *Nucleons with Chiral Loops*, *Nucl. Phys. B* **307** (1988) 779.
- [5] V. Bernard, N. Kaiser and U.-G. Meißner, *Chiral dynamics in nucleons and nuclei*, *Int. J. Mod. Phys. E* **4** (1995) 193 [hep-ph/9501384].
- [6] V. Bernard and U.-G. Meißner, *Chiral perturbation theory*, *Ann. Rev. Nucl. Part. Sci.* **57** (2007) 33 [hep-ph/0611231].
- [7] V. Bernard, *Chiral Perturbation Theory and Baryon Properties*, *Prog. Part. Nucl. Phys.* **60** (2008) 82 [arXiv:0706.0312 [hep-ph]].
- [8] T. R. Hemmert, B. R. Holstein and J. Kambor, *Chiral Lagrangians and  $\Delta(1232)$  interactions: Formalism*, *J. Phys. G* **24** (1998) 1831 [hep-ph/9712496].
- [9] N. Fettes and U.-G. Meißner, *Pion - nucleon scattering in an effective chiral field theory with explicit spin 3/2 fields*, *Nucl. Phys. A* **679** (2001) 629 [hep-ph/0006299].
- [10] J. Beringer,  *$\pi N \rightarrow \pi\pi N$  scattering in chiral perturbation theory*, *PiN Newslett.* **7** (1992) 33.
- [11] V. Bernard, N. Kaiser and U.-G. Meißner, *The Reaction  $\pi N \rightarrow \pi\pi N$  at threshold*, *Phys. Lett. B* **332** (1994) 415, [Erratum-ibid. **B 338**, 520 (1994)] [hep-ph/9404236].
- [12] V. Bernard, N. Kaiser and U.-G. Meißner, *The Reaction  $\pi N \rightarrow \pi\pi N$  at threshold in chiral perturbation theory*, *Nucl. Phys. B* **457** (1995) 147 [hep-ph/9507418].
- [13] T. S. Jensen and A. F. Miranda, *Low-energy single pion production processes  $\pi N \rightarrow \pi\pi N$* , *Phys. Rev. C* **55** (1997) 1039.
- [14] N. Fettes, V. Bernard and U.-G. Meißner, *One loop analysis of the reaction  $\pi N \rightarrow \pi\pi N$* , *Nucl. Phys. A* **669** (2000) 269 [hep-ph/9907276].
- [15] V. Bernard, N. Kaiser and U.-G. Meißner, *The Reaction  $\pi N \rightarrow \pi\pi N$  above threshold in chiral perturbation theory*, *Nucl. Phys. A* **619** (1997) 261 [hep-ph/9703218].
- [16] N. Mobed, J. Zhang and D. Singh, *Pion-induced pion production in heavy-baryon chiral perturbation theory*, *Phys. Rev. C* **72** (2005) 045204.
- [17] D. Siemens, V. Bernard, E. Epelbaum, H. Krebs and U. G. Meißner, *The reaction  $\pi N \rightarrow \pi\pi N$  in chiral effective field theory with explicit  $\Delta(1232)$  degrees of freedom*, *Phys. Rev. C* **89** (2014) 065211 [arXiv:1403.2510 [nucl-th]].
- [18] V. Pascalutsa and D. R. Phillips, *Effective theory of the  $\Delta(1232)$  in Compton scattering off the nucleon*, *Phys. Rev. C* **67** (2003) 055202 [nucl-th/0212024].
- [19] N. Fettes, U.-G. Meißner, M. Mojžiš and S. Steininger, *The Chiral effective pion nucleon Lagrangian of order  $p^4$* , *Annals Phys.* **283** (2000) 273, [Erratum-ibid. **288**, 249 (2001)] [hep-ph/0001308].
- [20] H. Krebs, A. Gasparyan and E. Epelbaum, *Chiral three-nucleon force at  $N^4 LO$  I: Longest-range contributions*, *Phys. Rev. C* **85** (2012) 054006 [arXiv:1203.0067 [nucl-th]].

- [21] H. Krebs, A. Gasparyan and E. Epelbaum, *Chiral three-nucleon force in effective field theory with explicit  $\Delta(1232)$  degrees of freedom I: Longest-range contributions at  $N^3 LO$* , to appear.
- [22] V. V. Vereshagin, S. G. Sherman, A. N. Manashov, U. Bohnert, M. Dillig, W. Eylich, O. Jakel and M. Moosburger, *Analysis of data on low-energy  $\pi N \rightarrow \pi\pi N$  reaction. I. Total cross-sections*, *Nucl. Phys. A* **592** (1995) 413 [hep-ph/9504361].
- [23] M. Kermani *et al.* [CHAOS Collaboration], *Exclusive measurements of  $\pi^{+-} p \rightarrow \pi^+ \pi^{+-} n$  near threshold*, *Phys. Rev. C* **58** (1998) 3419.
- [24] J. B. Lange, F. Duncan, A. Ambardar, A. Feltham, G. Hofman, R. R. Johnson, G. Jones and M. Pavan *et al.*, *Determination of the  $\pi^{+-} p \rightarrow \pi^+ \pi^+ n$  cross-section near threshold*, *Phys. Rev. Lett.* **80** (1998) 1597.
- [25] B. Long and V. Lensky, *Heavy-particle formalism with Foldy-Wouthuysen representation*, *Phys. Rev. C* **83** (2011) 045206 [arXiv:1010.2738 [hep-ph]].
- [26] S. Prakhov *et al.* [Crystal Ball Collaboration], *Measurement of  $\pi^- p \rightarrow \pi^0 \pi^0 n$  from threshold to  $p(\pi^-)$  750-MeV/c*, *Phys. Rev. C* **69** (2004) 045202.

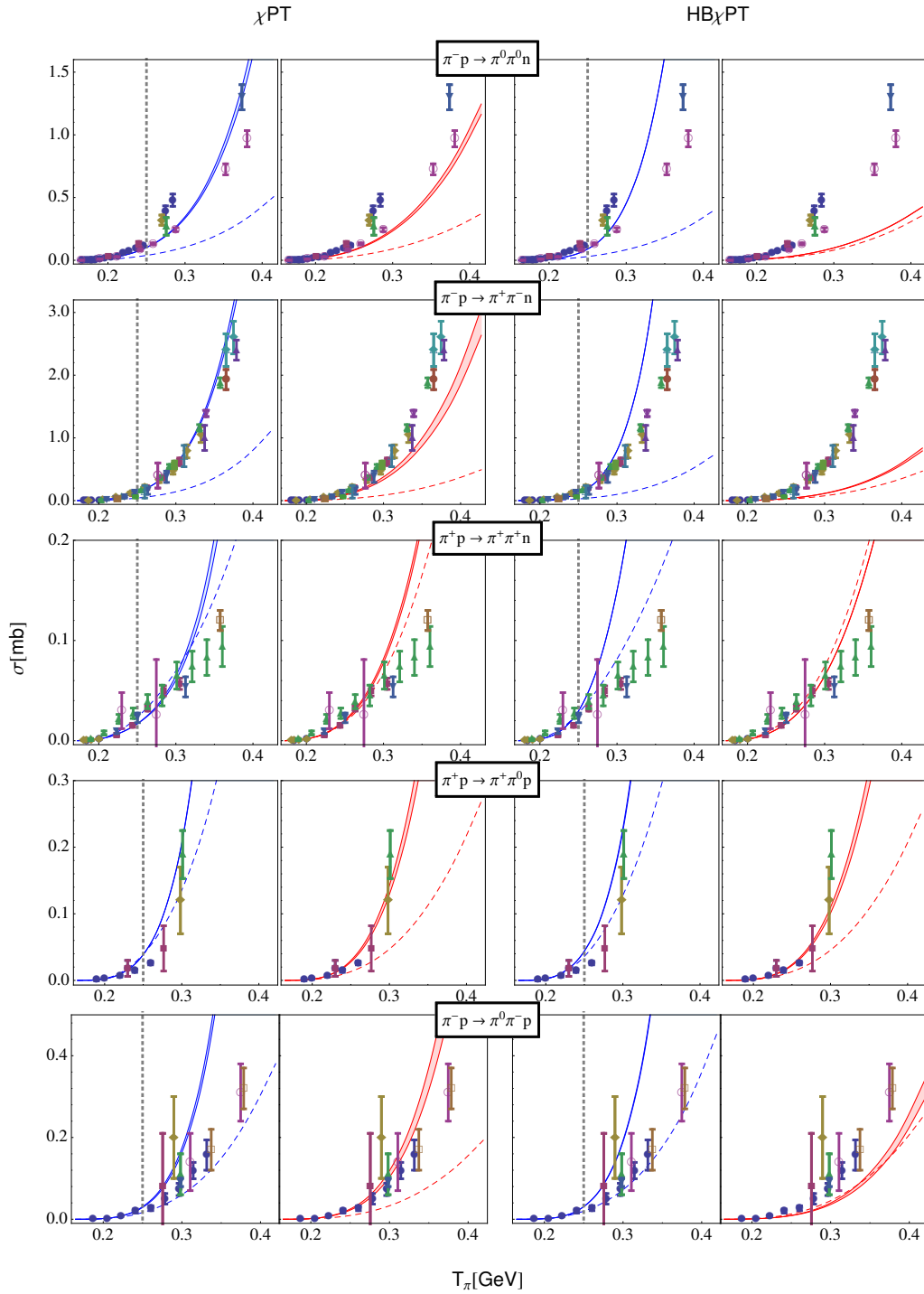


**Figure 2:** Predictions for the total cross section up to  $T_\pi \simeq 400$  MeV. The columns from left to right correspond to the  $\Delta$ -full covariant,  $\Delta$ -less covariant,  $\Delta$ -full HB and  $\Delta$ -less HB  $\chi$ PT predictions, respectively. The dashed lines and solid bands refer to leading-order and next-to-leading-order results. The bands correspond to using the KH and GW sets of LECs  $c_i$ . The energies used in the fit are below the vertical dotted line.



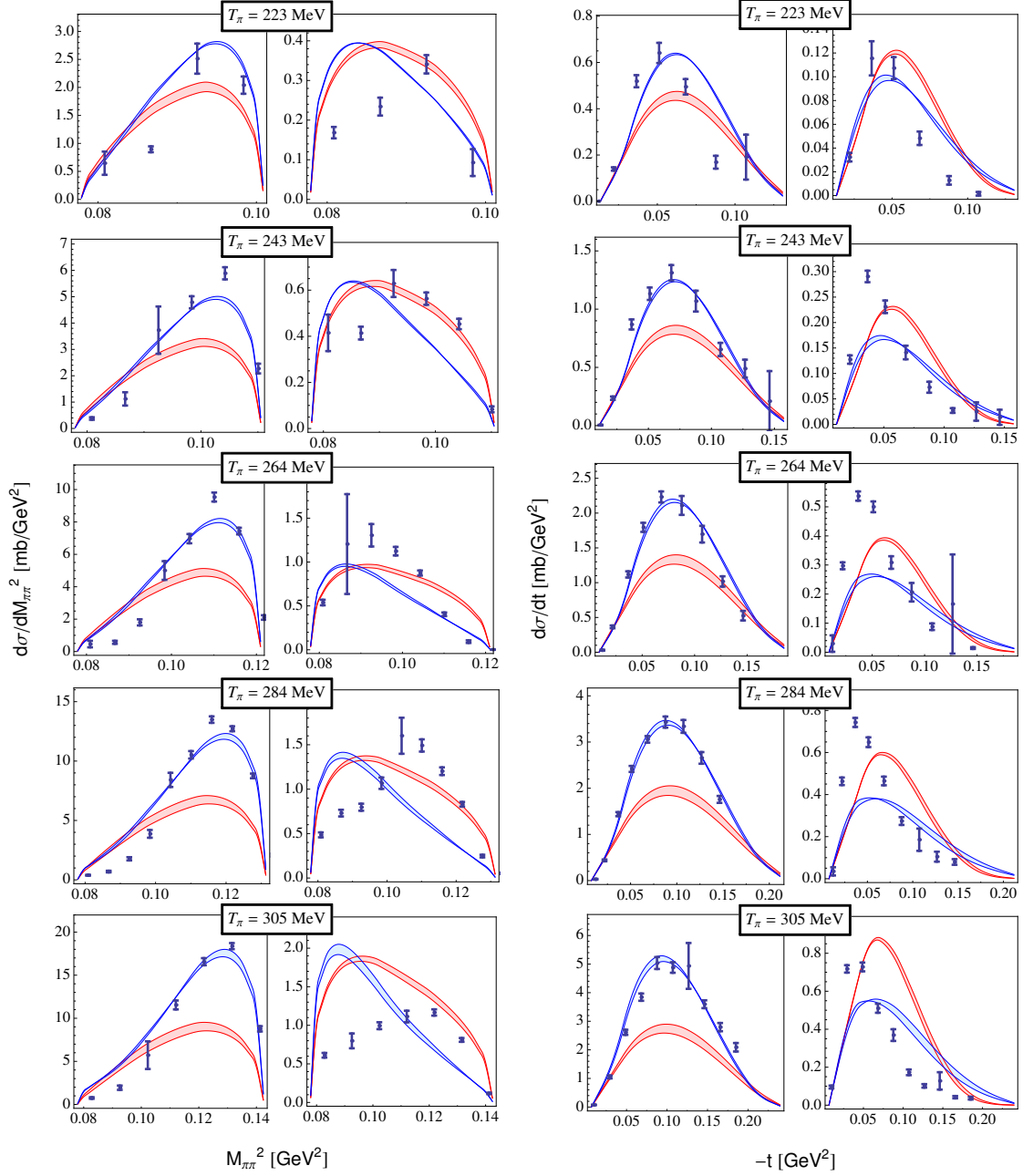


**Figure 3:** Comparison of next-to-leading-order covariant  $\Delta$ -full and  $\Delta$ -less  $\chi$ PT predictions for the single-differential cross sections with respect to  $M_{\pi\pi}^2$  and  $t$ , respectively, between the two channels  $\pi^- p \rightarrow \pi^+ \pi^- n$  (left) and  $\pi^+ p \rightarrow \pi^+ \pi^+ n$  (right). The red and blue bands refer to  $\Delta$ -less and  $\Delta$ -full calculations, respectively.